

# Enhanced cone penetration test interpretation with the Particle Finite Element method (PFEM)

## Interprétation améliorée des essais de pénétration au cône par la méthode des éléments finis des particules (PFEM)

L. Monforte

*Universitat Politècnica de Catalunya, Barcelona, Spain*

M. Arroyo, A. Gens

*Universitat Politècnica de Catalunya, Barcelona, Spain*

J.M. Carbonell

*International Centre for Numerical Methods in Engineering (CIMNE), Barcelona, Spain*

**ABSTRACT:** The paper presents an enhanced interpretation of the cone penetration test based on numerical analysis performed using the Particle Finite Element Method (PFEM). This method allows the incorporation of strong non-linearities, notably those associated with the large displacements and strains arising from the process of the penetration of the cone. Realistic constitutive laws can also be used. Undrained CPT tests are analysed using a single phase formulation whereas CPTu tests are examined using a two-phase formulation that allows the computation of pore pressures and the study of partially drained tests. It can be concluded that PFEM provides an efficient and robust method to analyse insertion problems that are ubiquitous in geotechnical engineering.

**RÉSUMÉ:** L'article présente une interprétation améliorée des essais de pénétration au cône basée sur une analyse numérique effectuée à l'aide de la méthode des éléments finis des particules (PFEM). Cette méthode permet l'incorporation de fortes non-linéarités, notamment celles associées aux grands déplacements et aux déformations résultant du processus de pénétration du cône. Des lois de comportement réalistes peuvent également être utilisées. Les tests CPT non drainés sont analysés à l'aide d'une formulation à une seule phase, tandis que les tests CPTu sont examinés à l'aide d'une formulation à deux phases qui facilite le calcul des pressions interstitielles et l'étude des essais partiellement drainés. On peut en conclure que PFEM constitue une méthode efficace et robuste pour analyser les problèmes d'insertion omniprésents en géotechnique.

**Keywords:** Cone penetration test; in-situ testing; permeability; Particle FEM

## 1 INTRODUCTION

The cone penetration test (CPT) is one of the prime means of soil investigation. The interpretation of the tests – establishing the link between cone measurements and constitutive parameters

of the soil - is still based on empiricism or the solution of simplified problems (for instance, cavity expansion).

More rational interpretation charts might be developed based on results of the numerical simulation of the CPT as a boundary value problem

using realistic governing equations and constitutive models. The simulation of this insertion problem is however a complex task due to the large number of strong non-linearities involved related to the constitutive equation, the contact problem as well as those arising from the large strain formulation. Although the Finite Element method may cope with all these non-linearities, a major obstacle is mesh distortion that leads to numerical inaccuracies and, in some cases, it may stop the computation. The Particle Finite Element method is able to overcome this limitation by employing a particle discretization of the domain. Additionally, since the solution is computed with the Finite Element method, the method allows the use of complex constitutive models able to reproduce realistically the stress-strain and strength behaviour of the soil.

In the paper, the method is first applied to the cone penetration test (CPT) under undrained conditions to assess the effect of steel-soil contact roughness on the cone resistance and sleeve friction. An extension of the method to two-phase conditions allows the consideration of pore pressures and effective stresses necessary for a proper reproduction of piezocone (CPTu) tests. Now the effects of penetration rate, partial drainage and, again, cone roughness on cone resistance and sleeve friction can be readily examined.

## 2 NUMERICAL APPROACH

The numerical code G-PFEM (Geotechnical Particle Finite Element method) is an extension of PFEM specifically developed for the analysis of large strain contact problems in geomechanics (Monforte et al, 2017, 2018a). PFEM (Oñate et al, 2004, 2011) was originally proposed to tackle fluid-structure interaction problems. PFEM is a particle-based method that is supported by a mesh: the domain is discretized with a set of scattered particles and the solution is computed with a finite element mesh, the nodes of which are the particles. The finite element mesh is constantly re-triangulated with low order elements in order

to alleviate the problems that arise when the mesh becomes highly distorted. In addition, h-adaptive techniques are employed to obtain a better discretization in areas of the domain with large plastic deformation (Rodriguez et al, 2017).

To introduce the contact constraints between the soil and the structure, a penalty approach is used. The structure is assumed rigid; this hypothesis is adequate when the Young's moduli ratio between the structure and the soil is large (Sheng et al, 2005).

A typical solution algorithm, sketched in Figure 1, involves the following steps (Oñate et al, 2004):

1. Discretize the domain with a Finite Element mesh. Define the shape and movement of the rigid structure.
2. Identify the external boundaries. Search the nodes that are in contact with the rigid structure.
3. Compute some time-steps of the (hydro)-mechanical problem.
4. Construct a new FE mesh. This step may include re-triangulation of the domain, introduce new particles in an adaptive fashion and interpolate state variables between the previous mesh and the newly created one.
5. Go back to step 2 and repeat the solution process for the next time-steps.

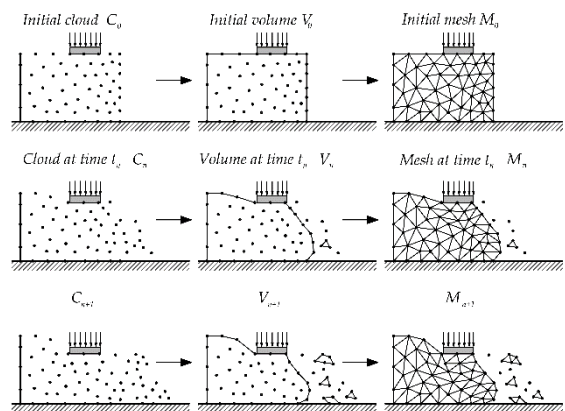


Figure 1. Scheme of a PFEM computational cycle

### 3 SINGLE PHASE FORMULATION

In a purely undrained case the soil can be considered as a single phase medium and only the linear momentum balance equation (i.e. equilibrium) needs to be solved. Accordingly, a total-stress Tresca constitutive model has been adopted to represent the soil whereas the tangential contact with the rigid cone has been simulated with a von Mises yield criterion. The analyses presented here have been performed with a rigidity index,  $I_r = 100$ .

Figure 2 shows the results of the cone penetration analyses in terms of the cone factor,  $N_{kt}$ , and the friction sleeve resistance; different values of the cone-soil adhesion ratio,  $\alpha$ , have been used, ranging from 0 to 0.7. As expected, the friction sleeve resistance coincides with the specified adhesion and the cone resistance increases modestly with the value of adhesion. In these simulations, a clear stationary state is identified after a penetration of about 20 radii.

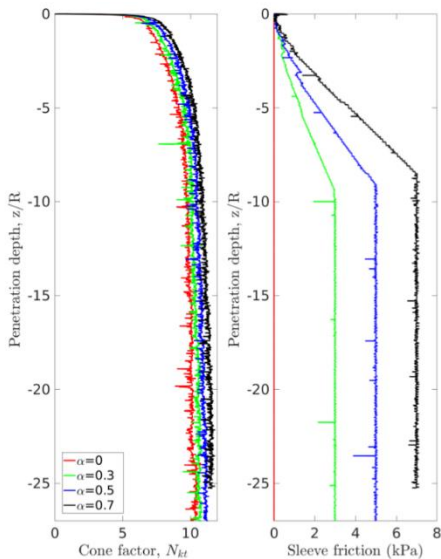


Figure 2. Cone factor and friction sleeve resistance for different values of adhesion. Total stress analysis

There has been much previous work on the simulation of this problem that has been widely used for benchmarking purposes of large-strain

total-stress numerical codes. The net cone resistance for the smooth case obtained using G-PFEM is well within the range obtained using other computational methods (Monforte et al, 2017).

The accuracy of the proposed approach is also assessed for the rough contact cases: the gradient of the variation of the cone factor as adhesion increase is 1.8, in good agreement with previous analyses (Figure 3).

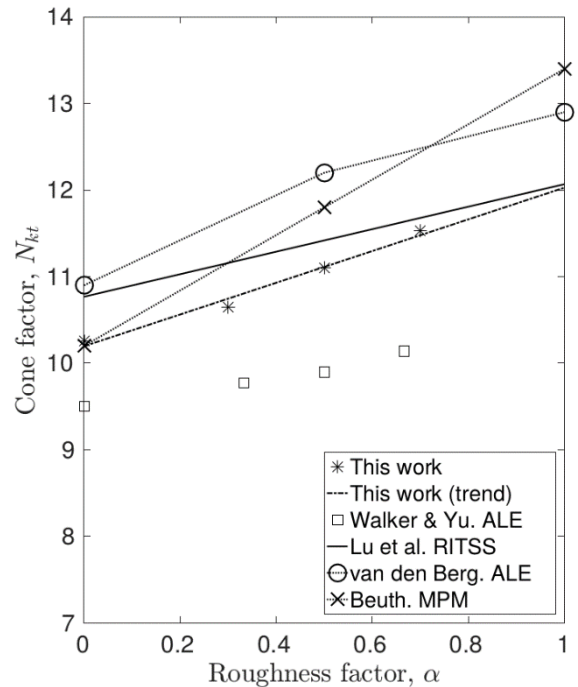


Figure 3. Influence of contact roughness on cone factor.

### 4 TWO-PHASE FORMULATION

In order to study the full range of partially drained conditions, the formulation has been extended to deal with the coupled hydromechanical problem. In this way, soil constitutive models can be expressed in terms of effective stress. Now, the governing equations are the equilibrium equation plus the balance of mass of the porous medium.

This section reports a parametric analysis in which a CPTu with standard dimensions is pushed into a Modified Cam Clay soil. In this particular case, the constitutive equation is written by using a hyperelastic version of the model (Houslby, 1997; Borja et al, 1997). The basic constitutive parameters are listed in Table 1. OCR is 1.2, i.e. a lightly overconsolidated clay is considered.

Table 1. Constitutive parameters adopted for the two-phase simulation of the CPTu

$e_0$	$\kappa$	$\lambda$	$M$	$\nu$	$p_c$ (kPa)	$K_0$
2.0	0.05	0.3	1	0.3	70	0.5

A sketch of the domain is presented in Figure 4. The computation starts with the cone pre-installed at a depth of 3 cone radii and a stress boundary condition of 57.5 kPa is placed on the top of the domain to simulate some soil depth. Drainage is only allowed through the bottom boundary of the soil domain.

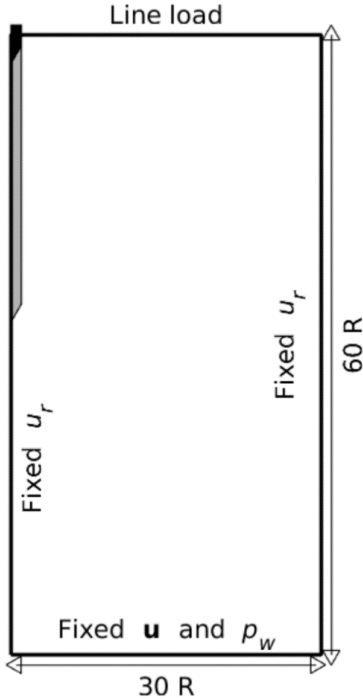


Figure 4. Sketch of the geometrical and boundary conditions.

#### 4.1 CPTu in partially drained conditions

In this section, the effect of partially drained conditions is analysed assuming a smooth interface behaviour in the cone-soil interface. To illustrate the effect of permeability on the cone metrics (net tip resistance,  $q_n$ , and excess water pressure), Figure 5 plots the values at steady state in terms of the normalized penetration velocity:

$$V = v D / c_v \quad (1)$$

where  $v$  and  $D$  are the cone velocity and diameter respectively whereas  $c_v$  stands for the coefficient of consolidation of the soil

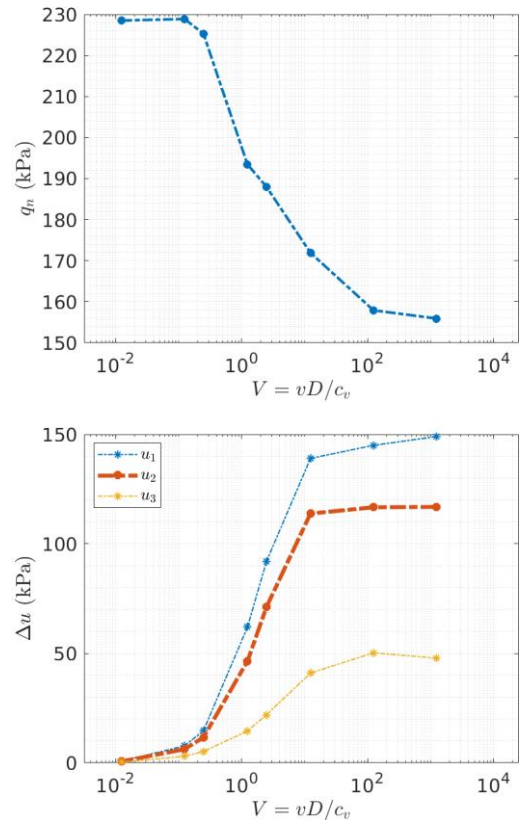


Figure 5. Evolution of cone metrics in terms of the normalized penetration velocity,  $V$ . (a) Net cone resistance, and (b) excess water pressure at three measurement locations.

The net cone resistance and excess water pressure for the two cases with the smallest permeabilities ( $k = 10^{-7}$  m/s and  $k = 10^{-8}$  m/s) are almost coincident; consequently, undrained conditions

may be assumed. On the other hand, at the highest value of permeability ( $k = 10^{-3}$  m/s), no excess pore pressure is generated. In drained conditions, the net cone resistance is 47% larger than in undrained conditions.

The excess water pressure at the mid-face of the cone ( $u_1$  location) is a 20% larger to that of the  $u_2$  position; whereas the measurement at the  $u_3$  location is much lower than the other two.

#### 4.2 Effect of the interface friction angle

The previous CPTu analyses have been repeated, this time considering different friction angles at the cone-soil interface,  $\delta$ , of  $10^\circ$ ,  $20^\circ$  and  $25^\circ$ . Consequently, the maximum allowable tangential stress at the cone-soil interface is:

$$|\boldsymbol{t}| < \tan(\delta) \sigma'_n \quad (2)$$

where  $\sigma'_n$  is the normal effective stress acting on the interface.

Figure 6 presents the effect of interface friction angle on the backbone curve. The curve describing the evolution of the excess water pressure at the  $u_2$  position (normalized by its value during undrained conditions) is not affected by the value of the interface friction angle: the somewhat erratic influence of the friction at the undrained end is likely due to numerical reasons.

The net cone resistance (normalized by its value during undrained condition) increases as the penetration rate gets closer to drained conditions. Additionally, the ratio between drained to undrained resistance increases as higher interface friction angles are considered.

Figure 6 also includes the backbone curves proposed by DeJong and Randolph (2012). These curves -based on results of cavity expansion, experimental data and finite element analysis of cone penetration- show a very good agreement with the numerical results reported here. Previous numerical analysis (Yi et al, 2012) have shown that the ratio between the drained and undrained net cone resistance increases as the stiffness ratio

( $G/p'$ ) increases. The parametric analysis reported here shows that the interface friction angle also plays a prominent role on the ratio between the cone resistance in drained and undrained conditions.

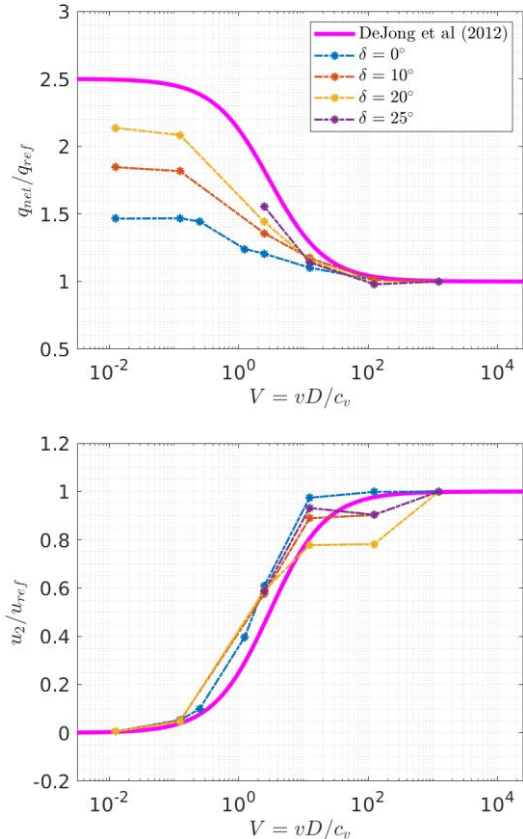


Figure 6. Effect of interface friction angle on the backbone curves for CPTu in Modified Cam Clay: (a) cone tip resistance, and (b) excess pore pressure at the  $u_2$  location.

To characterize the effect of the interface behaviour on the sleeve friction resistance, Figure 7 shows the effect of the interface friction ratio,  $\mu = \tan(\delta)$ , on the sleeve friction resistance for the two extreme permeability conditions (fully drained and undrained penetrations). For this particular set of constitutive parameters, this measurement appears independent of the hydraulic conditions. The stress state along the shaft of the

cone -particularly the  $\tau_{rz}$  component of the Cauchy stress tensor- does depend in fact on the hydraulic conditions. However, the integral of  $\tau_{rz}$  along the friction sleeve yields a similar value irrespectively of the hydraulic regime.

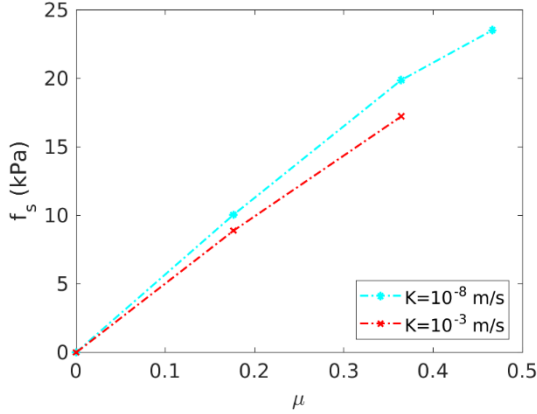


Figure 7. Influence of the interface friction ratio,  $\mu = \tan(\delta)$ , for completely drained and undrained conditions on the friction sleeve resistance.

### 4.3 Representation of the numerical results in interpretation charts

One of the major applications of CPTu is the determination of soil stratigraphy and the identification of soil type (Robertson, 2009). This is accomplished using charts that relate cone parameters (e.g. net tip resistance, friction sleeve, water pressure) to soil behaviour type.

Robertson (1990) developed a soil behaviour type identification method based on the following dimensionless metrics: normalized cone tip resistance, normalized water pressure and normalized friction ratio, defined as:

$$Q_t = q_n / \sigma'_{v0} \quad (3)$$

$$B_q = \Delta u_2 / q_n \quad (4)$$

$$F_r = f_s / q_n \quad 100 \% \quad (5)$$

More recently, Schneider et al (2008) proposed a new interpretation chart that allows the separation of the effect of partial consolidation from

that of the yield stress ratio. To this end, they developed a  $\Delta u_2 / \sigma'_{v0} - Q_t$  graph.

In Robertson charts, results from the numerical simulations lie in zone 3 and classify as ‘clays – clay to silty clay’ (Figures 8a and 8b).

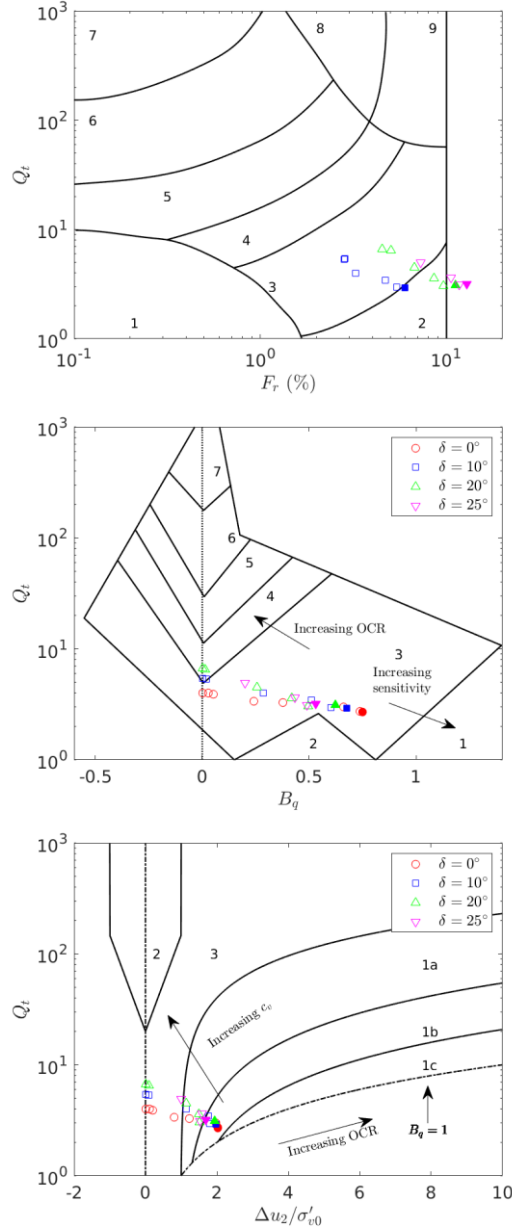


Figure 8. Numerical results depicted in custom interpretation charts: (a) and (b) Robertson (1990), and (c) Schneider et al (2008). Filled markers correspond to undrained results.

The numerical results in partially drained conditions agree well with the chart developed by Schneider et al (2008): results follow the predicted trend of increasing coefficient of consolidation (Figure 8c). The numerical results move from clays (zone 1b) to silts (zone 1a) and then to transitional soils (zone 3)

## 5 CONCLUSIONS

This contribution describes an ongoing effort to develop a code, based on the Particle Finite Element method, able to simulate the cone penetration test in clayey soils and other insertion problems in geotechnical engineering.

A parametric analysis has been reported, in which the effect of permeability and interface friction angle has been explored. The numerical results have been plotted in current practice interpretation charts; results lie in the regions expected for clays.

In this respect, it is worth noting that several application of the methodology described here are currently being developed. For instance, G-PFEM has been used to perform a detailed analysis of the so-called on-the-fly methods, in which permeability can be directly estimated from CPTu data streams without the need for any stoppage (Monforte et al. 2018b). More generally, PFEM provides an efficient and robust method to analyse insertion problems that are ubiquitous in geotechnical engineering.

## 6 ACKNOWLEDGEMENTS

This work has been supported by the Ministry of Science and Innovation of Spain through research grant BIA2017-84752-R.

## 7 REFERENCES

Borja, R.I., Tamagnini, C., Amorosi, A. 1997. Coupling plasticity and energy-conserving

elasticity models for clays. *J. Geotech. Geoenviron. Engng* **123**(10), 948-957.

DeJong, J.T., Randolph, M.R. 2012. Influence of partial consolidation during cone penetration on estimated soil behavior type and pore pressure dissipation measurements. *J. Geotech. Geoenviron. Engng* **138**(7), 777-788.

Houlsby, G.T. 1985. The use of a variable shear modulus models for clays. *Computers and Geotechnics* **1**(1), 3-13.

Monforte, L., Arroyo, M., Carbonell, J.M., Gens, A. 2017. Numerical simulation of undrained insertion problems in geotechnical engineering with the particle finite element method (PFEM). *Computers and Geotechnics* **82**, 144-156.

Monforte, L., Arroyo, M., Carbonell, J.M., Gens, A. 2018a. Coupled effective stress analysis of insertion problems in geotechnics with the particle finite element method (PFEM). *Computers and Geotechnics* **101**, 114-129.

Monforte, L., Arroyo, M., Gens, A., Carbonell, J.M. 2018b. Hydraulic conductivity from CPTu on-the-fly: a numerical evaluation. *Géotechnique Letters* **8**(4) doi.org/10.1680/jgele.18.00108

Oñate, E., Idelshon, S.R., Del Pin, F., Aubry, R. (2004) The particle finite element method – an overview *Int. J. Comput. Methods*, **1**(2), 267-307.

Oñate, E., Idelshon, S.R., Celigueta, M.A., Rossi, R., Marti, J., Carbonell, J.M., Ryzakov, P., Suárez, B. 2011. Advances in the particle finite element method (PFEM) for solving coupled problems in engineering. In *Particle-Based Methods*, pp 1-34. The Netherlands: Springer.

Robertson, P.K. 1990. Soil classification using the cone penetration test. *Can. Geotech. J.* **27**(1), 151-158.

Robertson, P.K. 2009. Interpretation of cone penetration tests – a unified approach. *Can. Geotech. J.* **46**(11), 1337-1355.

Rodriguez, J.M., Carbonell, J.M., Cante, J.C., Oliver, J. 2017. Continuous chip formation in

metal cutting processes using the Particle Finite Element method (PFEM). *Int J Solids Struct.* **120**, 81-102.

Schneider, J.A., Randolph, M.F., Mayne, P.W., Ramsey, N.R. 2008. Analysis of factors influencing soil classification using normalized piezocone tip resistance and pore pressure parameters. *J. Geotech. Geoenviron. Engng.* **134**(11), 1569-1586.

Yi, J.T. Goh, S.H., Lee, F.H., Randolph, M.F. 2012. A numerical study of cone penetration in fine-grained soils allowing for consolidation effects. *Géotechnique.* **62**(8), 707-719.